11

Unified model for intraplate earthquakes

PRADEEP TALWANI

Abstract

After the development of plate tectonic theory, understanding the genesis of intraplate earthquakes has been the focus of many studies. I combine the results of these studies with recently improved seismological and other data to formulate a unified model for intraplate earthquakes. Intraplate earthquakes occur within continental interiors in response to a generally uniform, compressional stress field associated with large-scale tectonic forces. The global pattern of seismic energy release occurs preferentially in failed and passive rifts, and less frequently on the edges of cratons. Thermo-mechanical modeling shows that during basin inversion, rifts preferentially utilize inherited zones of crustal weakness. As a result, pockets of elevated strain rate and consequently local stress accumulations occur on discrete structures, which I identify as local stress concentrators (LSC). These are located in both the upper and lower crust within the rift, and their reactivation occurs in the present-day compressional stress field in the form of intraplate earthquakes. Commonly observed LSCs are favorably oriented (relative to the regional stress field) fault bends and intersections, compressional stepovers, flanks of shallow plutons and buried rift pillows. Stress build-up associated with one or more LSCs interacts with, and produces a potentially detectable local rotation of the regional stress field with wavelengths of tens to hundreds of kilometers. A local rotation of the regional stress field provides evidence of local stress increase, and thus potentially suggests the location of future intraplate earthquakes.

11.1 Introduction

Although intraplate earthquakes (IPE) are associated with only about 5% of global seismic energy release, historically these earthquakes account for a disproportionate number

Intraplate Earthquakes, ed. Pradeep Talwani. Published by Cambridge University Press.

of deaths and destruction (www.earthquake.usgs.gov/earthquake/world/most_destructive.php). The earliest attempt to explain IPEs on a global scale was by Sykes (1978), who noted that due to a sparsity of seismic stations and short historical records the nature of IPEs was not well understood. Over the past four decades, since the development of the theory of plate tectonics, which explains nearly 95% of the Earth's seismic energy release near or along plate boundaries, there have been continuing improvements in the quality and quantity of data associated with IPEs. These include the development of improved techniques in locating IPEs with better instrumentation and denser seismic networks; paleoseismology to document prehistoric earthquakes; global positioning systems to detect minute earth movements; *in situ* stress measurements; improved geophysical techniques, especially seismic tomography; mathematical models to explore various hypotheses; and improved analytical techniques to process various types of data. Improvements in observational data have been accompanied by the formulation of explanatory models which fall into two groups. The first were aimed at explaining the seismicity at a particular location, the New Madrid seismic zone (NMSZ) in the United States in particular. Most of these were conceptual in nature and are generally not testable. The second were based on global observations of geological and mechanical similarities, and spatial association between geological features and seismicity. However, a unified model for the genesis of IPEs has been missing.

Among the global observations are the apparent affinity of IPEs to rifted regions (Johnston and Canter, 1990), and the association of IPEs with identifiable geological features, e.g., with buried plutons (Long, 1976), fault bends (King, 1986) and rift pillows (Zoback and Richardson, 1996). These earthquakes occur due to reactivation caused by a regional, uniform compressional stress field (Zoback, 1992a). Simultaneously, sedimentologists developed basin inversion models to show how reactivation of elongate rift structures produces the sedimentary basins in central Europe (Ziegler, 1987; Nielsen *et al*., this volume). Finally, *in situ* stress measurements and analysis of seismicity data revealed that in the vicinity of some of these earthquakes the local maximum horizontal stress field was rotated (Zoback and Richardson, 1996). These different observations and explanations were akin to the proverbial description of an elephant by blind men, each examining one part of the elephant's anatomy. I show that these observations, hypotheses, and ideas are not mutually exclusive, rather they are all different parts of a synoptic view. In this chapter I consider these earlier observations and integrate them with newer observations, data analyses, and mathematical models to develop a unified model for IPEs. In this testable model, the main idea is that IPEs are associated with stress build-up at local stress concentrators (LSC) due to a uniform, far-field regional stress field associated with plate tectonic forces. These LSCs were formed in and are preferentially located in former rift zones, and their reactivation occurs by the present-day compressive stress fields in the mid-continental regions. I will refer to this phenomenon as "reactivation by stress inversion." This stress accumulation causes detectable changes in the nature and direction of the regional stress field in their vicinity over wavelengths of tens to hundreds of kilometers.

In the first part I describe the results of earlier studies, which are then integrated to arrive at the new model. I start with a description of ideas about the present-day lithospheric stress field in continental regions (Section 11.2), and how it is perturbed on regional (Section 11.3) and local (Section 11.4) scales. Perturbation on a local scale and the resulting local rotation of the stress field attest to the presence of the LSCs (Section 11.5). The magnitudes of the local stress perturbations are discussed in Section 11.6. In Section 11.7, I address the global distribution of IPEs, and in Section 11.8 I use insights from basin inversion modeling to develop the unified model, presented in Section 11.9. Some consequences and uses of this model are discussed in Section 11.10, and the conclusions are presented in the final section.

11.2 Lithospheric stress field

In her seminal study, Mary Lou Zoback (1992a) identified two orders of stress in the continental lithosphere. The first-order mid-plate stress field, extending uniformly over thousands of kilometers, S_T, is associated with plate tectonic forces. Ziegler (1987) showed that collision-related major stresses can be transmitted over great distances through continental and oceanic lithosphere. This continental stress is generally compressional with one or both horizontal stresses (S_{Hmax} and S_{hmin}) greater than the vertical stress, S_V. In a compressional regional stress field, the maximum horizontal stress, S_{Hmax}, can be determined by direct measurements at shallow depths and its direction inferred from focal mechanisms at seismogenic depths. Zoback (1992a) showed that in continental interiors the direction of S_{Hmax} is the same at both depth ranges. Superimposed on S_T are second-order stress fields with wavelengths of hundreds to thousands of kilometers associated with specific geological and tectonic features. Following Zoback (1992a), the near-surface perturbing horizontal deviatoric stress above the LSC is labeled S_L (compression is assumed positive). Locally, this superposition of S_T with S_L can cause a local rotation of the regional stress field. The vertical stress due to the regional or local stress perturbation does not cause stress rotation, but can change the relative stress magnitude (stress regime, Zoback, 1992a). Rotation of the horizontal stress field depends on the angle between S_T and (the axis of) the local structure as well as on the relative magnitudes of S_T and S_L. For a potentially detectable rotation of S_T ($\sim 15°$) the magnitude of the local horizontal uniaxial stress, S_L, must be greater than about half the magnitude of the horizontal stress difference ($S_{Hmax} - S_{hmin}$). Zoback (1992a) showed that discernible rotations of S_T implied that the magnitudes of both S_T and S_L were of the same order, hundreds of megapascals.

11.3 Regional perturbation of the stress field S_T

11.3.1 Early ideas about perturbing lithospheric stresses

Before the development of plate tectonics theory, different lithospheric stresses were identified as potential causes of IPEs. We recognize them now as the second-order perturbing

stresses described by Zoback (1992a). These stresses have also been incorporated in more recent models.

Artyushkov's (1973) suggestion that lithospheric stresses were caused by inhomogeneities in regional and global thickness led Mareschal and Kuang (1986) to speculate on the role of topography and density heterogeneities in the genesis of IPEs. Turcotte and Oxburgh (1976) hypothesized that IPEs were associated with tensional failure in the lithosphere caused by intraplate stresses generated by different processes. These processes included changes in latitude of surface plates (membrane stresses), change in temperature with depth (thermal stresses), addition or removal of overburden, changes in crustal thickness, in addition to the forces associated with the driving mechanism for plate tectonics. The role of addition and removal of overburden and associated thermal stresses was emphasized further by Haxby and Turcotte (1976).

11.3.2 Perturbation of S_T by surface and other processes

The regional compressive stress field due to plate tectonic forces, S_T, can be perturbed on both a regional scale due to surface or other processes, and on a local scale due to stress build up near LSCs. At many locations of IPEs, S_T is perturbed by a regional stress field due to surface processes, such as deglaciation, erosion, and sedimentation (see, e.g., Talwani and Rajendran, 1991; Muir-Wood, 2000; Mazzotti *et al*., 2005) or, as suggested by modeling, by stress transfer to the brittle upper crust of thermal and other stresses caused by thermal and compositional anomalies in the lower crust and upper mantle (Liu and Zoback, 1997; Kenner and Seagall, 2000; Pollitz *et al*., 2001; Sandiford and Egholm, 2008). For example, Liu and Zoback (1997) suggested that the higher heat flow within the NMSZ resulted in thermal weakening of the lower crust and upper mantle and the higher ductile strain rates led to stress concentrations. The transmission of these stresses to the upper crust leads to the observed seismicity. Kenner and Segall (2000) speculated that sudden tectonic perturbations and viscous relaxation of a weak lower crust within an elastic lithosphere caused stress transfer to the overlying crust and the resulting seismicity. Perturbation on a regional scale can advance or delay the occurrence of an IPE and also alter the style of the deformation and its location. They further modeled that coseismic slip in the crustal faults in turn reloads the lower crust, causing cyclic stress transfer and thus accounting for large repeat earthquakes.

11.3.3 Deglaciation and erosion

Of these various suggestions for regional stress perturbation, the role of surface processes, especially deglaciation, has been investigated by many authors.

Deglaciation occurred most rapidly around 10,000 years ago and melting was largely complete by about 6,000 years ago. The crust is still reacting to glacial unloading of the former ice sheet as it rebounds to a state near isostatic equilibrium (e.g., Steffen and Kaufmann, 2005). This is manifested by uplift in the deglaciated regions in northern

latitudes. Stein *et al*. (1979), Quinlan (1984), Hasagawa and Basham (1989), and Wu (1998), among others, suggested that as a result of glacial isostatic adjustment (GIA), stresses accumulated during loading can be released by a reduction of the normal stress due to the upward flexure of the lithosphere due to the removal of the surface load. Wu (1998) estimated that the contribution of GIA towards fault instability in Laurentia and Fennoscandia is a few MPa, in agreement with Zoback's (1992b) estimate of ~10 MPa. Wu and Johnston (2000) estimated that, because the flexural stresses decay rapidly from the ice margin, deglaciation has no effect hundreds of kilometers away from the edge of the ice sheet. They estimated that its influence on the seismogenic regions in Eastern Canada was <0.5 MPa, and concluded that the magnitude of post-glacial stress is too small to trigger the M8 earthquake near New Madrid, contrary to the conclusion of Grollimund and Zoback (2001).

In a related study, Calais *et al*. (2010) suggested that the seismicity in the NMSZ results from stress changes caused by the upward flexure of the lithosphere associated with river incision in the northern Mississippi Embayment. In their model the removal of ~6 m of sediments over a 60 km wide area between 16 and 12 kyr BP, and another 6 m of sediments over a 30 km wide area between 12 and 10 kyr BP imposed additional tension stresses (<0.5 MPa) at depths between 5 and 15 km. Calais *et al*. (2010) suggest that these stress changes were adequate to trigger the 1811–1812 sequence of M ~ 7 earthquakes on critically stressed faults in the NMSZ.

Pollitz *et al*. (2001) proposed that the seismicity results from the downward pull of the brittle upper crust by a suddenly sinking mafic body. According to this hypothesis, sinking began several thousand years ago due to perturbations in the lower crust related to the last North American glaciation.

11.3.4 Unverifiable models

Most of the above models are generally not testable since they are based on unverifiable assumptions. For example, as Calais *et al*. (2010) point out, there is no evidence of a weak lower crust or a sinking high-density body, as was suggested by Pollitz *et al*. (2001). Also, the magnitudes of the perturbing stresses associated with these models are about an order of magnitude lower than those of the regional stress field. However, I will show that they do contain some plausible elements, and can play a role in altering the stress regime at higher latitudes. Those will be incorporated in the unified model.

11.4 Local perturbation of the regional stress field: local stress concentrator models

The observation of a spatial association of seismicity locations with structures delineated by geophysical and geological data led to the suggestion of a causal relation between the two. The seismicity locations were inferred to be associated with local stress build-up, S_L, on structures due to S_T. From elasticity theory (e.g., Jaeger and Cook, 1979) a far-field stress

is concentrated by a heterogeneity with a different elastic modulus than the surrounding space. The same is true for faults, which are equivalent to planar heterogeneities. Three types of LSCs were identified and incorporated into a testable local stress concentrator model for intraplate earthquakes by Talwani and Gangopadhyay (2000). These are shallow plutons, rift pillows, and fault intersections and kinks. These are described below.

11.4.1 Stress amplification around plutons

A spatial association between seismicity and stress accumulation on the periphery of mafic and ultramafic plutons embedded in felsic country rocks was identified by Long (1976), Kane (1977), and McKeown (1978), and ascribed as being due to rigidity contrast between the two. Analytical modeling by Campbell (1978) showed that the accumulated differential stress was largest when an elliptical inclusion was parallel to S_T, and it scaled with the size of the pluton. McKeown (1978) also noted that ancient rift zones may be a primary control on the locations of mafic intrusions.

With increasingly better seismic, geophysical, and geological data, a spatial association between seismicity and stress accumulation on the periphery of plutons was observed in the NMSZ (Hildenbrand *et al*., 2001), and in South Carolina (Stevenson *et al*., 2006; Talwani and Howard, 2012). Agreement of calculated stresses on the periphery of plutons, and the predictions of the analytical model of Campbell (1978), with the observed locations of seismicity has further strengthened the suggestion of a causal association between the two (Stevenson *et al*., 2006).

11.4.2 Seismicity associated with rift pillows

A rift pillow forms as a result of mafic magmatic intrusion into the lower crust during rift formation. In failed rifts this high-density rift pillow forms in the lower crust and the excess mass of the pillow must be supported by the strength of the cooled lithosphere, inducing deviatoric stresses in the plate (Zoback and Richardson, 1996). A causal association of seismicity with buried rift pillows has been inferred in Brazil, in the NMSZ, and at two locations in India.

The east–west trending Amazonas rift in central Brazil is one of the largest continental rifts in the world (Zoback and Richardson, 1996). Two deep (23 km and 45 km) moderate (M 5.1 and 5.5) earthquakes occurred on the northern margin of the rift in 1963 and 1983. Based on the theoretical models by Sonder (1990) and Zoback (1992a), Zoback and Richardson (1996) suggested that these earthquakes were associated with local stress concentration around the rift pillow at those depths. The depth of the rift pillow was inferred from gravity data. The observed direction of the maximum horizontal stress, S_{Hmax}, in the vicinity of the rift inferred from bore-hole data and from focal mechanisms was found to be rotated $\sim$75° counter-clockwise relative to the east–west direction of S_T. Based on modeling, they suggested that the induced rift normal stresses, S_L, associated with the rift pillow can be as large as the tectonic stress, and that its influence on S_T depends both on the orientation of the rift pillow relative to S_T and on the ratio of the magnitude of the two stresses.

Seismic refraction data indicate the presence of a buried high-density rift pillow in the lower crust beneath the NMSZ (Mooney *et al*., 1983). Grana and Richardson (1996) modeled the local stress field associated with a rift pillow at a depth of 30 km beneath the NMSZ. They found that the direction of S_{Hmax} near the top of the rift axis was rotated clockwise ~10° to 30° relative to S_T. They suggested that the perturbed stress field over this and other stress pillows was adequate to trigger earthquakes.

In their study of the M 5.8 1997 Jabalpur earthquake in central India, Rajendran and Rajendran (1998) concluded that this deep earthquake (36 ± 4 km) located within the Narmada rift was associated with a rift pillow at that depth. The presence of the rift pillow has been inferred from gravity, deep seismic sounding, and seismic reflection data (Rajendran and Rajendran, 1998).

Mandal (2013) analyzed 10 years of aftershocks of the 2001 Bhuj earthquake occurring in the Kutch rift zone He inverted more than 450 well-determined focal mechanisms in 10 km depth slices to obtain the directions of the local stress orientations. While the orientation of S_{Hmax} for the top 30 km was along the regional direction of S_T, ~N–S, he found that for the depth range of 30–40 km it was rotated clockwise by ~50°. The results of seismic tomography suggested that the earthquakes at that depth were possibly associated with fluid-filled mafic intrusions (rift pillow?).

In an alternative explanation for the role of a rift pillow in contributing to seismicity in NMSZ, Stuart *et al*. (1997) suggested that the cause of the observed seismicity was the stress concentrated in a weak sub-horizontal detachment fault in the lower crust directly above the rift pillow.

11.4.3 Stress concentration associated with fault geometry: the (fault) intersection model

It has been known for a long time that fault bends play an important role in the generation and termination of seismicity (see, e.g., King, 1986). With improving seismicity data the role of fault intersections in generating earthquakes was recognized. In the intersection model (Talwani, 1988) intersecting faults form a locked volume where stress builds up in response to S_T. This stress build-up can be large enough to cause major earthquakes. Fault intersections provide locations for the initiation and cessation of rupture and for the local generation and accumulation of stress and the resulting earthquakes (Talwani, 1999). The observed pattern of seismicity is consistent with the results of numerical analyses of the stress fields in the immediate vicinity of fault intersections (Andrews, 1989; Jing and Stephansson, 1990).

Simple 2D numerical models have been used to investigate the response to intersecting faults corresponding to known geological features subjected to far-field loading (Gangopadhyay *et al*., 2004; Gangopadhyay and Talwani, 2005). These studies focused on the NMSZ and the Middleton Place Summerville seismic zone near Charleston, South Carolina. The resultant stress patterns, sign and amplitude of the maximum shear stress were consistent with the observed locations and structural style of faulting. These numerical models thus support the hypothesis that in a localized volume of previously weak crust, fault

intersections act as stress concentrators that give rise to seismicity in their vicinity. Parametric studies by Gangopadhyay and Talwani (2007) showed that a fault at 45° ± 15° relative to S_{Hmax}, with an intersecting fault at 90° ± 35°, to it are optimal directions for stress accumulation. This model is scale independent, and has been found applicable in explaining many cases of IPE. On a continental scale, Hildenbrand *et al*. (1996, 2001) observed that along the 400 km long Reelfoot Rift axis, the only seismically active zone, the NMSZ, occurs near the 100 km wide intersection zone of the Reelfoot Rift and the Missouri batholiths. Perhaps the first regional-scale field evidence of stress concentration or perturbation in the vicinity of intersecting tectonic features was provided by Ellis (1991). By mapping stress distribution from 1,500 hydraulically fractured wells in south-central Oklahoma, he found a spatial correlation between the intersection of major crustal fault zones, the resulting stress distribution, and the contemporary seismicity. In another example, Dentith and Weatherstone (2003) also found that the spatial and temporal distribution of seismicity associated with the M 6.9 Meckering earthquake in southwestern Australia closely correlated with the predictions of the intersection model.

Many strike-slip fault systems consist of numerous discrete en echelon segments. Another geometrical configuration that acts as a local stress concentrator is a restraining stepover in an en echelon strike-slip fault system. Two-dimensional quasi-static elastic analysis of the restraining stepovers by Segall and Pollard (1980) showed that they store elastic energy and may be the sites of large earthquakes. We recognize them as potential local stress concentrators. Association of these stopovers with seismicity has been observed in the Middleton Place Summerville seismic zone near Charleston, South Carolina (Talwani, 1999), the NMSZ (Figure 7.11) and the 2001 Kutch earthquake (Figure 6.1).

11.4.4 Local shear model

Iio *et al*. (2004) presented a conceptual "local shear" model to explain the large recurring IPEs in Japan. They assumed that a seismogenic fault in the brittle crust extends as a ductile fault zone with low viscosity into the viscoelastic lower crust. This assumption was based on their inference of aseismic slip (localized shear deformation) on the downward extensions of seismogenic faults following several earthquakes (Iio and Kobayashi, 2002). In their conceptual model, plate tectonic forces load the crustal fault and can cause (intraplate) earthquakes. The stress drop that follows subsequently loads the fault extension in the viscoelastic lower crust. When the stress in the lower crust relaxes, it reloads the fault in the upper crust, which is further loaded by S_T, leading to the next earthquake. The recurrence time of the earthquakes in the brittle crust is a function of the viscosity of the lower crust and the strength of the brittle fault. The presence of fluids can drastically reduce the strength of the fault. This model presents a simple mechanism for transmitting stresses from the ductile lower crust to the brittle upper crust, and may be applicable to the models discussed earlier.

11.4.5 Local stress concentrator model

Talwani and Gangopadhyay (2000) suggested that one or more of the three LSCs, fault intersections, shallow plutons, and buried rift pillows were associated with most intraplate earthquakes. Gangopadhyay and Talwani (2003) examined seismicity, geophysical, and geological data for 20 $M \geq 5.0$ intraplate earthquakes to identify the responsible LSCs. They found that fault intersections were associated with 30% of the events, fault intersections and plutons together with 35%, i.e., fault intersections were associated with nearly two-thirds of the events. Plutons alone and rift pillows alone were associated with 20% and 15% of the events, respectively. In the following section I examine some examples that provide evidence for the presence of local stress anomalies within the uniform regional tectonic stress field.

11.5 Evidence of the presence of a local stress anomaly

Zoback (1992a) identified large-scale regional crustal features as sources of second-order stress fields. Because of superposition of S_T by these regional stresses, the resultant stress field with wavelengths of hundreds to thousands of kilometers is rotated relative to the direction of S_T. Now, with the availability of modern seismic networks, stress field perturbations associated with LSCs and the resulting rotations of S_T with wavelengths of tens to hundreds of kilometers are being recognized and thus providing evidence for their presence. The orientation and magnitude of the anomalous stress build-up in a discrete volume around a LSC, S_L, and the resulting local rotation, γ, of the S_T depends on the kind of stress concentrator and its geometrical relationship with S_T (Figure 11.1).

For a rift pillow, Sonder (1990) and Zoback (1992a) showed that γ depends on the angle, α, between the strike of the rift and S_T, and the ratio of the differential horizontal stress to S_L, $(S_{Hmax} - S_{hmin}) / S_L$. The magnitude of S_L depends on the mass contrast with the surrounding volume (Figure 11.1b). For intersecting faults, S_L is oriented along the direction of the shorter of the two intersecting faults (BC in Figure 11.1c) and γ depends on the angle, α, between the longer fault AB and S_T and the angle between the two faults, β. The magnitude of S_L depends on the lengths of the two faults and the angles α and β (Gangopadhyay and Talwani, 2007). For plutons, the directions of S_L and γ depend on the orientation of the long axis of an elliptical pluton relative to S_T (Figure 11.1d). The magnitude of S_L depends on the size of the pluton and the ratio of its rigidity modulus to that of the surrounding volume (Campbell, 1978). Next we present some examples of stress rotation associated with LSCs (see also Table 11.1). Due to uncertainties in the determination of the orientation of S_L from seismicity data, only those cases with $\gamma \geq 15°$ are considered meaningful (Mazzotti and Townend, 2010).

11.5.1 France

In a reanalysis of 40 years (1962–2002) of shallow crustal seismicity (≤12 km) data from western and central France, including 4,500 events, four with M 5.1 to 5.7, Mazarbaud *et al.*

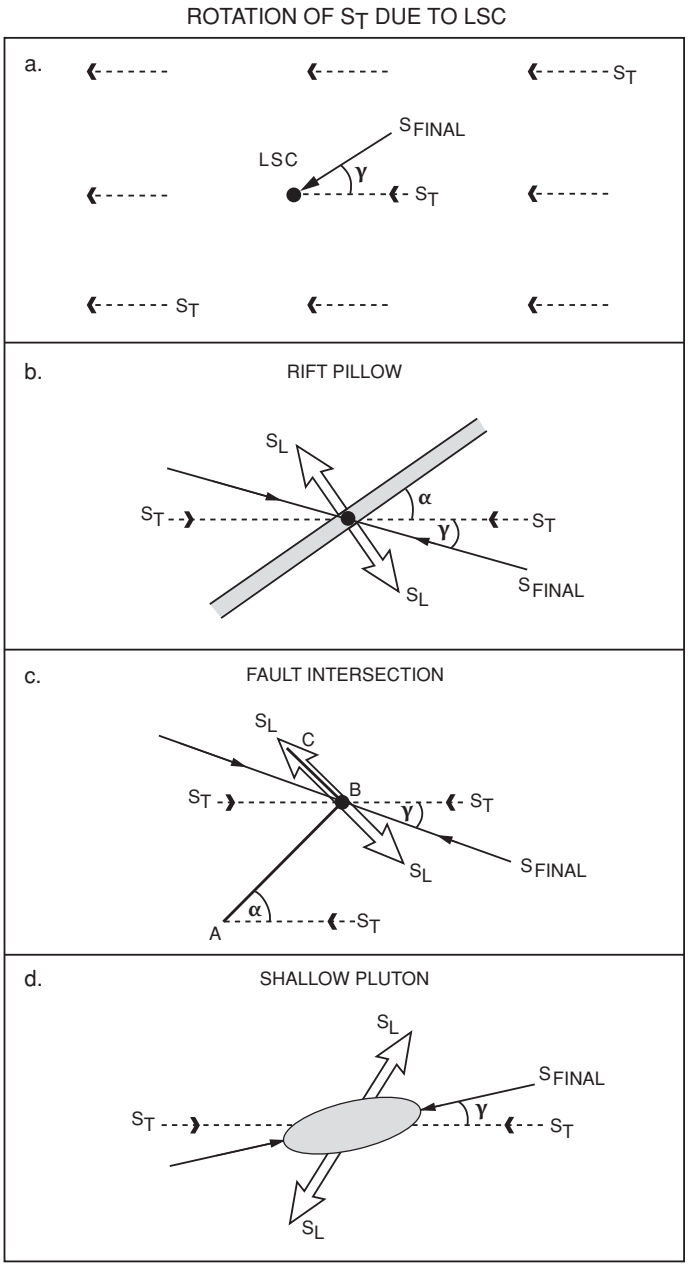

Figure 11.1 The stress field due to a local stress concentrator, S_L, causes a rotation of the regional stress field, S_T, by $\gamma°$ to S_{FINAL}. (a) In a continental setting, S_T is perturbed only in the vicinity of a LSC (solid circle). (b) The rift pillow (solid circle) lying within the rift (shaded area) oriented at an angle $\alpha°$ to S_T. (c) For intersecting faults AB and BC, S_L lies along shorter fault BC. The longer fault AB is oriented at an angle $\alpha°$ to S_T. (d) For a shallow pluton (shaded) S_T is rotated towards S_L.

Table 11.1 *Rotation of local S_{Hmax}*

Location seismic zone	Stress rotation angle (°) (+ cw)	Lateral extent km × km	References
Central-Western France			Mazarbaud *et al*. (2005)
N. Armorican Massif	39	~50–100	
S. Armorican Massif	5*	120 × 350	
E. Massif Central	24*	200 × 250	
Charente	17	~50–100	
Southeastern France			Baroux *et al*. (2001)
Rhone Valley	−8*	110 × 230	
Moyenne Durance FZ	0	70 × 210	
Digne Nappe reverse faulting domain	62	50 × 90	
Digne Nappe normal faulting domain	38*	30 × 70	
SE of Argentera Massif	−3*	80 × 120	
Ligurian basin	−43	50 × 200	
Eastern North America			Mazzotti and Townend (2010)
Lower St. Lawrence	44	100 × 300	
Charlevoix NW	1	20 × 40	
Charlevoix SE	47	20 × 40	
Gatineau	−5	150 × 200	
Ottawa	−8	100 × 450	
Montreal	14	100 × 150	
N. Appalacian	32	150 × 400	
C. Virginia	48	80 × 150	
E. Tennessee	−4	100 × 250	
NMSZ	6	100 × 300	
Northeastern Canada			Steffen *et al*. (2012)
Hudson Bay	~−45	~300 × 600	
Japan			Kawanishi *et al*. (2009)
Southwest Japan	20	35 × 250	
Brazil			Zoback and Richardson (1996)
Amazonas (rift pillow)	−75	~150 wide	
United States			Grana and Richarson (1996)
NMSZ (rift pillow)	10–30	~80 wide	
India			Mandal (2013)
Kutch (rift pillow)	~50	~10s	
NMSZ			Horton *et al*. (2005)
Bardwell, Kentucky	40	~60	

* Relative to direction of S_{Hmax} in local extensional stress regime.

(2005) found evidence of perturbation of S_T by local sources. They found that a regionally significant strike-slip regime with a northwest-trending S_{Hmax} was rotated at two locations and overprinted by local extensional perturbations at two others with wavelengths of tens to hundreds of kilometers. Mazarbaud *et al*. (2005) related the extensional deviatoric stress at the Eastern Massif Central (Table 11.1) to an underlying bulging of the crust at the apex of the hot mantle plume, inferred from seismic tomography.

In a similar study Baroux *et al*. (2001) determined the local stress regime near Provence in southeastern France by inverting focal mechanism data. They found evidence for short-scale (tens of kilometers) variations in the direction of S_{Hmax} close to the major faults in three locations. Significantly different stress regimes were detected, both compressional and extensional. The direction of the compressional stress was found to be both parallel and rotated relative to S_T.

11.5.2 Eastern North America

Mazzotti and Townend (2010) inverted focal mechanisms to determine the local state of stress in ten seismic zones in central and eastern North America. They compared the azimuth of the seismically determined S_{Hmax} with S_T obtained from relatively shallow boreholes within 250 km of the seismic zones. For four seismic zones the two azimuths were essentially parallel. However, a statistically significant clockwise rotation of ~30–50° was found for the Charlevoix, Lower St. Lawrence, and Central Virginia seismic zones, and to a lesser extent for the North Appalachian seismic zone (Table 11.1). The stress rotation occurs over distances of 50–100 km for the Lower St. Lawrence, Central Virginia, and northern Appalachian seismic zones and 20–40 km for the Charlevoix seismic zone. The Charlevoix seismic zone consists of two clusters, the northwest cluster with seismically determined S_{Hmax} parallel to S_T, and the southwest cluster where it is rotated clockwise 47°. The northwest cluster lies beneath the northern shore of the St. Lawrence River, with the southwest cluster beneath the river. Seismic tomography results show that the 5–10 km wide aseismic gap between the two clusters is associated with a high seismic velocity body (Vlahovic *et al*., 2003).

The results of stress inversion of thrust focal mechanisms for five post-2007 (M 3.6–4.1) and three earlier (M 5.0–6.2) earthquakes in the Hudson Bay region of northeastern Canada show that locally the S_{Hmax} strikes NNW–SSE, in contrast with the regional NNE–SSW direction (Table 11.1; Steffen *et al*., 2012). The authors attribute this counter-clockwise rotation of S_{Hmax} to the presence of a roughly E–W oriented fault zone and its combined effect with the regional perturbation due to glacial isostatic adjustment and the regional stress field S_T.

11.5.3 Japan

Kawanishi *et al*. (2009) examined earthquakes occurring over a 10-year period with $M \geq 1.0$ and depths ≤ 30 km in the Chogochu district of southwest Japan. Using inversions

of focal mechanisms obtained from a dense network of seismic stations, they found the azimuth of S_{Hmax} in the ~250 km long and ~35 km wide seismically active belt lying along the Japan Sea coast. In this seismic belt, where three $M \geq 7.0$ earthquakes had occurred earlier, they found that the S_{Hmax} was rotated ~20° clockwise with respect to the S_T direction in the adjacent ~330 km long and 140 km wide area (Table 11.1). Based on modeling, the authors attribute the stress rotation to the deformation of an aseismic fault or a ductile fault zone in the lower crust beneath the seismic belt.

11.5.4 Continental rift zones

Some examples of stress rotation associated with buried rift pillows were described in Section 11.4b above. They vary from ~75° counter-clockwise for the Amazonas basin to ~50° clockwise for the Kutch rift zone (Table 11.1).

11.5.5 Bardwell, Kentucky, earthquake sequence

With increasing improvements in seismic monitoring, it now has become possible to detect stress rotations inferred from analysis of smaller earthquakes. The M 4 June 2003 Bardwell, Kentucky, earthquake and its aftershocks were recorded on a dense network (Horton *et al*., 2005). Stress inversion of very accurately determined focal mechanisms reveal that locally (to ~60 km) S_T is rotated 40° clockwise (Table 11.1). The responsible LSC, however, was not identified by Horton *et al*. (2005).

11.6 Magnitude of local stress perturbations

In her analysis of the magnitude of various cases of regional secondary stresses with detectable rotations of S_T (i.e., $\gamma > 15°$), Zoback (1992a) showed that S_L must be greater than about half the regional horizontal stress difference, i.e., hundreds of megapascals. This suggests that, if a detectable stress field rotation is associated with a LSC, the magnitude of associated S_L needs to be of the same order, i.e. hundreds of megapascals. Mazzottii and Townend (2010) estimated the magnitudes of S_L associated with 30° to 50° rotation of S_T for the Lower St. Lawrence, Charlevoix, and Central Virginia seismic zones. Assuming that the responsible seismogenic structures were oriented perpendicular to S_L, and using Equation 8 of Zoback (1992a), they obtained an estimate of ~160 to 250 MPa for the differential stress in the horizontal plane at mid-crustal depths of ~8 km. This value was calculated based on an assumed coefficient of friction of $\mu = 0.8$, with near-hydrostatic pore pressures. The estimate of S_L reduces to 20 to 40 MPa for $\mu = 0.1$, or near-lithostatic pore pressure. However, the assumptions of such anomalous parameters are not compatible with recent analysis by Hurd and Zoback (2012), who suggest normal values of μ (0.6–0.8) and hydrostatic pore pressures, supporting the premise here that the stresses associated with LSCs that lead to moderate and large earthquakes are of the order of hundreds of megapascals.

In various models for the genesis of IPE discussed earlier, regional stress perturbations due to surface processes or due to anomalies in the lower crust and upper mantle (Section 11.3.3) are a few megapascals at best, at least an order of magnitude lower than the contribution of LSCs to the local stress perturbations. This magnitude difference suggests that, in the present-day stress field, local stress perturbations associated with LSCs are the likely cause of IPE rather than the smaller regional effect of surface processes, e.g., deglaciation and erosion. The latter could, however, provide a trigger for an earthquake. In the following section I examine the global distribution of IPEs and possible association with geological features.

11.7 Intraplate earthquakes and rifts

A possible spatial association between IPEs and rifts has been suggested by a number of earlier studies (see, e.g., Adams and Basham, 1989; Johnston, 1989). Johnston and Kanter (1990) found that globally most of the seismic energy release within intraplate regions occurs by the reactivation of weak pre-existing structures within failed rifts and passive margins in response to an ambient compressional stress field. Schulte and Mooney (2005) reevaluated this correlation by comparing an updated seismicity catalog with a compilation of "Rifts of the world" (Şengör and Natal'in, 2005). Using the latter's definition," Rifts are fault-bounded elongate troughs, under and near which the entire thickness of the lithosphere has been reduced in extension during their formation," Schulte and Mooney (2005) found that failed rifts and passive margins (labeled "interior rifts and rifted continental margins" by them) together accounted for more than half of all IPEs and 90% of the seismic energy release. Twelve taphrogens, which are linked chains of rifts and grabens in rifted continental crust, account for 74% of all events and 98% of the total seismic energy release within failed rifts. Gangopadhyay and Talwani (2003) found that IPEs not associated with old rifts occur primarily in Pre-cambrian crust.

11.7.1 Correlation with deep mantle structure

Mooney *et al*. (2012) used shear-wave velocity perturbation, δV_S, at a depth of 175 km as a proxy for lithospheric temperature and composition. δV_S is the perturbation in the measured shear-wave velocity with reference to the Preliminary Reference Earth Model (Dziewonsky and Anderson, 1981) and was interpreted in terms of cratonic and non-cratonic lithosphere. They explored possible correlations between the gradient of lithospheric thickness, interpreted from δV_S anomalies at 175 km depth, and intraplate seismicity with magnitudes $\geq$ 4.5. They concluded that significant crustal intraplate seismicity is concentrated in rifted margins (in agreement with Schulte and Mooney, 2005) and the edges of cratons as defined by seismic tomography (Figure 11.2). As detailed knowledge of the structures associated with IPEs in the cratonic regions of Australia, Brazil, China, and India improves, we will be able to identify the nature of the responsible LSCs. In the absence of such detailed knowledge, the LSCs associated with rift structures will be the focus of this study. In this

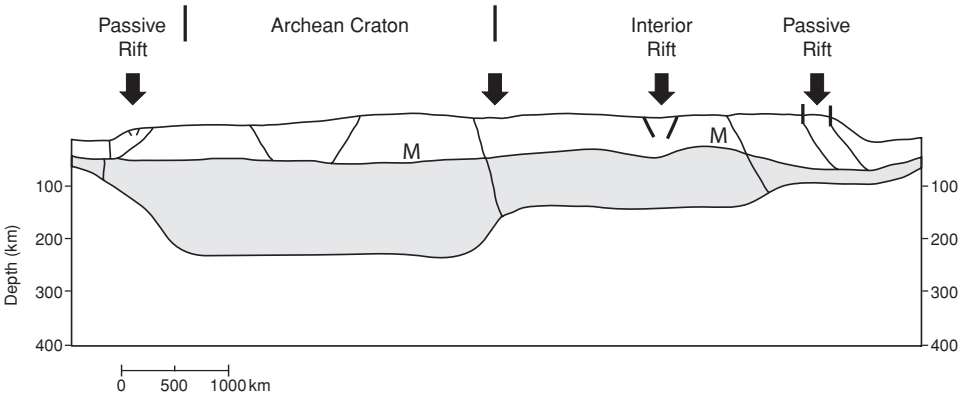

Figure 11.2 A schematic continental lithospheric cross-section. The primary locations of seismicity (solid arrows) are in rifts located along the passive margins and continental interior, and at the boundary of the deep Archean craton with the surrounding regions. The shaded area shows the lithosphere. M represents Moho. (Adapted from Mooney *et al*., 2012.)

chapter I will focus on the larger earthquakes ($M \geq 4, 5$) with rift association, realizing that nearly 40% of $M \geq 4.5$ events (Schulte and Mooney, 2005) and a significantly higher percentage of smaller events may have other causes.

According to my hypothesis, large IPEs occur by reactivation of faults in the present-day compressional stress field. Whether a fault within a rift will be reactivated depends on whether or not it is favorably oriented relative to S_T, its strength, its tectonic history and geometry. An intracratonic rift forms in response to plate margin processes. The resulting geometry is a series of half-grabens with alternating polarity along strike, separated by accommodation zones (e.g., Ziegler, 1987). Thus, the present configuration of the rift is the result of its tectonic history, and reactivation of structures within it depends on their orientation with respect to S_T. Insight into reactivation of structures within a rift by stress inversion can be provided by modeling, which is described next.

11.8 Insights from basin inversion modeling

The term "basin inversion" is used to describe the tectonic process in which the deep part of a sedimentary basin or continental rift reverses its vertical direction of movement and becomes uplifted (Ziegler, 1987; Nielsen and Hansen, 2000). An inversion zone is an elongate structure that has deformed in response to compression. Among different intraplate discontinuities within the rigid crust, rifts with a thinner crust are most prone to inversion in response to compressional stresses emanating from plate boundaries (Ziegler, 1987). Ziegler described many examples of these inversion zones in central Europe and speculated on their genesis. To investigate the mechanism of these inversion zones, Nielsen and Hansen (2000) developed a numerical thermo-mechanical model of basin inversion in response to a compressional intraplate stress field. The results of their model showed that a pre-existing

zone of structural and rheological weakness in a rift is the optimal location for reactivation under compressional inversion. These results suggested that pre-existing faults in a rift would be likely locations for reactivation. In a more detailed study Hansen and Nielsen (2003) developed a two-dimensional thermo-mechanical continuum model to investigate the whole sequence of lithospheric rifting and subsequent basin reactivation and inversion by compression. In this model, rifting was assumed to initiate from a thermal anomaly imposed at the base of the crust, with mass flux from below and above. The thermal anomaly is created by elevating the Moho temperature in a small area around the model center (Figure 11.3a). Allowing for strain hardening, the rifting process is carried out for 10 Ma during which boundary faults and interior conjugate faults extending to the brittle–ductile transition develop. The mantle undergoes regional uplift to compensate for localized crustal thinning and the development of crustal-scale faults significantly weakens the lithosphere and influences the rift structural style. Compressional stress is applied after 60 Ma and basin inversion follows as a natural consequence. In their reactivation model, the inversion preferentially utilizes the inherited zones of crustal weakness. After compression and post-compressional relaxation, at 100 Ma the modeled compressive strains are preferentially located along the boundary faults, interior through-going and conjugate faults, and on top of the up-welled mantle in the lower crust (Figure 11.3b). A comparison of the locations of these pockets of elevated strain rates (Figure 11.3b) with models showing seismicity and associated structures in the Sea of Japan (Figure 4 in Kato *et al*., 2009; and reproduced as Figure 9.5 in this volume) and the Kutch rift (Figure 4 in Biswas, 2005; modified and reproduced as Figure 6.3c in this volume) was used to infer the locations of LSCs within the rift (Figure 11.3c). The comparison led to the identification of a rift pillow (1), border faults and interior conjugate faults (2 and 3). A through-going fault to the lower crust based on the model by Iio *et al*. (2004) was added to the figure (4) together with a shallow pluton (5) based on the observation of the Osceola pluton in the NMSZ (Hildenbrand *et al*., 2001). Additionally, the rifts are broken and displaced laterally along transfer faults and compressional stepovers, providing additional fault intersections. Shallow plutons are emplaced at or near these intersections, producing more LSCs.

Next I will compare the results of this model with earlier models proposed to explain IPEs and with the global distribution of IPEs (Schulte and Mooney, 2005; Mooney *et al*., 2012) to formulate a unified model for intraplate earthquakes.

11.9 Unified model for intraplate earthquakes

11.9.1 The model

Some of the observations and conclusions presented in earlier sections can be summarized as follows:

- There is a generally uniform compressional stress field, S_T, in continental regions.
- Globally, IPEs occur primarily in rifts and at craton boundaries.
- Basin inversion models show how weak structures within a rift are preferentially reactivated by S_T.

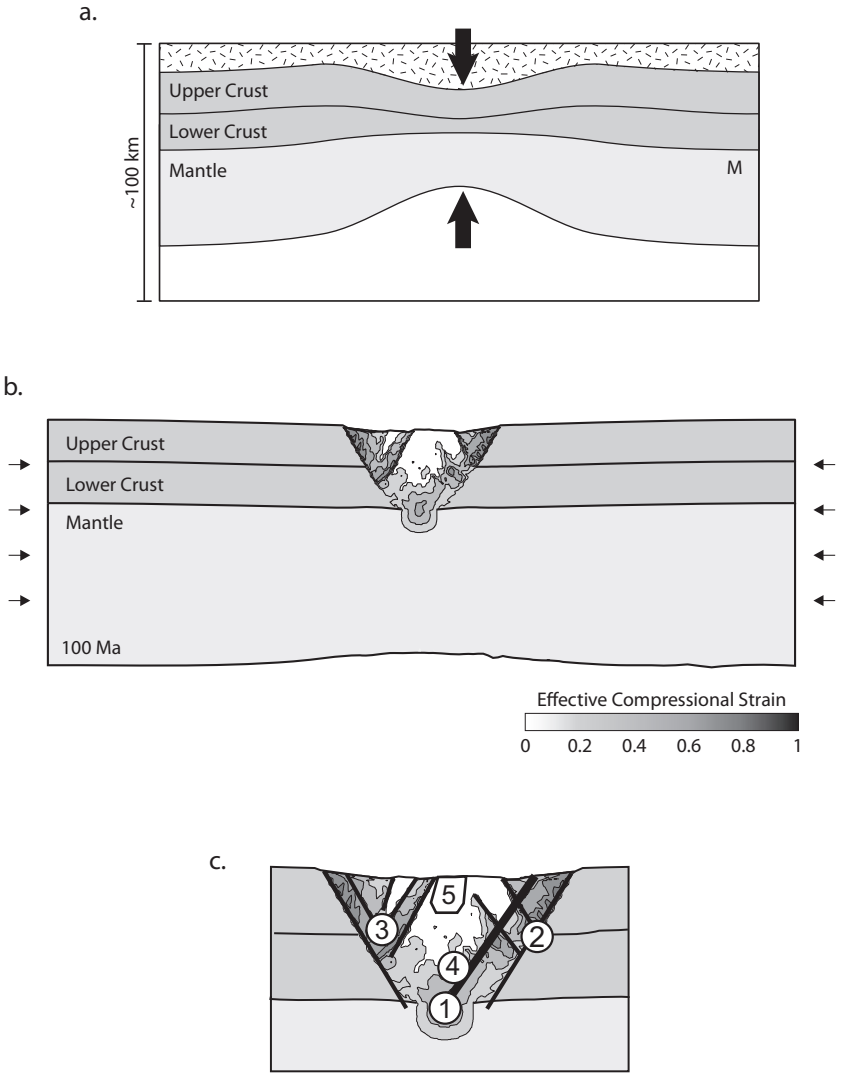

Figure 11.3 (a) The model set-up. A thermal anomaly is imposed at the base of the crust in the middle of the model. The stippled pattern shows sediments, and the arrows show mass flux. (b) Compressional strain-rate distribution after 100 Ma. The reactivation of weak rifted structures by stress inversion results in isolated locations of elevated strain rates (darker patterns). (c) Schematic figure showing interpreted locations of LSCs within the rift (this study). The regions of modeled high strain rates (darker pattern in (b)) were compared with locations of faults and rift pillows in the Kutch and Sea of Japan rift basins to infer the location of a rift pillow (1), border and interior conjugate faults (2 and 3). A through-going fault into the lower crust (4) is based on the model by Iio *et al.* (2004) and a shallow pluton (5) is based on the Osceola pluton within the NMSZ (Hildenbrand *et al.*, 2001). (Adapted from Hansen and Nielsen, 2003.)

- Within rifts, pockets of elevated modeled strains are identifiable with locations of LSCs.
- In response to S_T, around the LSC there is temporal accumulation of local stress, S_L, which can lead to IPEs.
- The influence of S_L extends over wavelengths of tens to hundreds of kilometers.
- An increase in S_L can cause a local rotation in the direction of S_T.
- The magnitude of S_L can be comparable to that of S_T, hundreds of megapascals.
- The structural style and timing of IPEs at any LSC can be modulated by the smaller second-order regional stresses such as those due to GIA, erosion, and lower crust–upper mantle thermal anomalies.

The observations and conclusions listed above address different aspects of IPEs and the factors that contribute to their genesis. Individually, most of these observations have been known for a long time. I combine them with the results of improved observational data to develop a testable, unified model for intraplate earthquakes.

Intraplate earthquakes occur in continental regions characterized by a uniform compressional stress field, S_T, extending over thousands of kilometers (Zoback, 1992a). This stress field is primarily associated with strike-slip faulting, i.e., $S_{Hmax} > S_V \geq S_{hmin}$ (e.g., in continental United States), unless perturbed by a secondary stress field due to regional or local features (Talwani and Rajendran, 1991; Zoback, 1992a, b). There is a global pattern of seismic energy release by IPEs in response to S_T. It preferentially occurs in failed (or interior) rifts and passive (or rifted) margins (see, e.g., Johnston and Kanter, 1990; Schulte and Mooney, 2005). Most of the seismic energy release not associated with failed rifts occurs on the edges of cratons (Mooney *et al*., 2012). Nearly half of the smaller IPEs ($M < 4.5$) occur outside the failed rifts, and their contribution to the global seismic energy release from IPEs is negligible (Schulte and Mooney, 2005). Consequently, in this model I will focus on the larger ($M \geq 4.5$) events.

Thermo-mechanical modeling by Hansen and Nielsen (2003) demonstrated that large strain accumulations are localized within rifts during their formation and reactivation. These high strain accumulations occur on discrete structures that act as local stress accumulators or concentrators. These LSCs are located in both the upper and the lower crust. Their reactivation in the form of IPEs occurs in the present-day compressional stress field. Commonly observed LSCs are favorably oriented, relative to S_T, fault bends and intersections, flanks of shallow plutons, and buried rift pillows (Talwani and Gangopadhyay, 2000; Gangopadhyay and Talwani, 2003). Local stresses build up on these discrete LSCs lying within the failed rifts or at the edge of cratons and cause IPEs. Next I explore some of the features of S_L and its bearing on the genesis of IPEs.

11.9.2 Build-up of S_L and sequential fault reactivation

Local stresses accumulate at the LSCs in response to the regional stress field S_T. At any LSC, the local stress, S_L, grows with time until it reaches a critical threshold, and interacts with S_T to generate an earthquake. At any time the stress accumulation can occur on

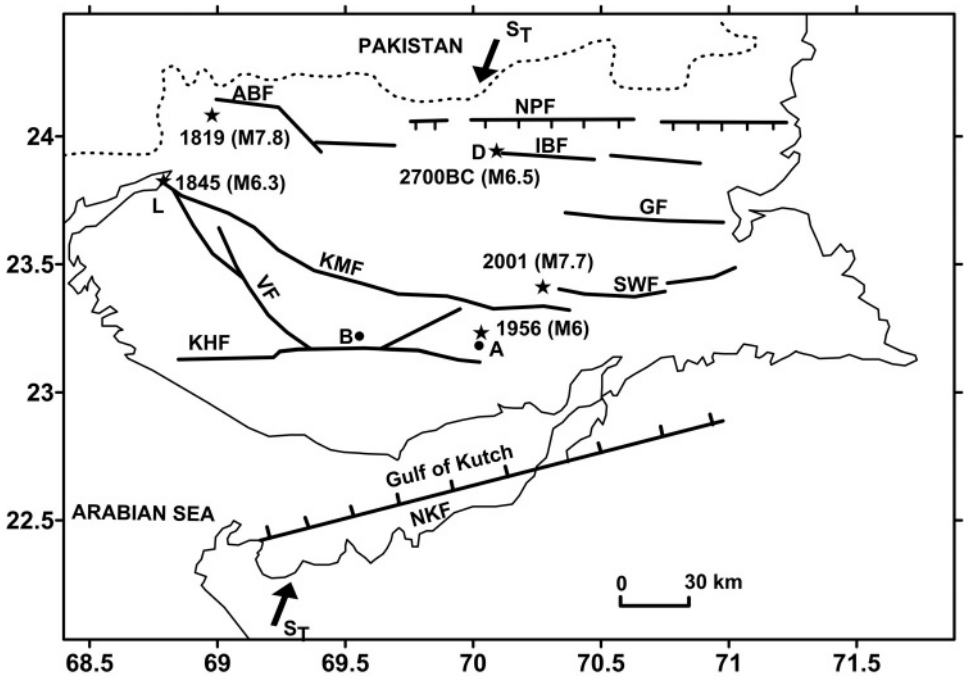

Figure 11.4 The Kutch Rift Basin lies between the Nagar Parkar and North Kathiawar faults (NPF and NKF). Historical earthquakes in 1819, 1845, and 2700 BC are inferred to be associated with the Allah Bund, Kutch Mainland, and Island Belt faults (ABF, KMF, and IBF) respectively. Instrumentally located 1956 Anjar (A) and 2001 Bhuj (B) earthquakes were associated with the Katrol Hill (?) and South Wagad faults (KHF and SWF) respectively. D and L show the locations of old historical towns at Dholavira and Lakhpat. S_T shows the direction of the regional S_{Hmax}. (Fault map courtesy B. K. Rastogi.)

one or more LSCs, and the release of this accumulated stress can occur sequentially. For example, within the Kutch Rift Basin destructive earthquakes have occurred on different faults (Figure 11.4). The 1819 M 7.8 earthquake occurred on the northern Allah Bund fault, the 1845 M 6.3 earthquake that destroyed Lakhpat on the Kutch Mainland fault, the 1956 M 6 Anjar earthquake on the Katrol Hill fault (?) and the 2001 M 7.7 Bhuj earthquake on the North Wagad fault (Rastogi *et al*., this volume). Based on paleo-archeological data and historical reports of the destruction of Dholavira, the 2700 BC earthquake (estimated M 6.5) was associated with the Island Belt fault (Bisht, 2011). The absence of repeat earthquakes on any one of these faults possibly explains the absence of major topographic features associated with repeat earthquakes within the same rift.

Within the Reelfoot Rift in the Central United States, there is paleoseismic evidence of two large earthquakes hundreds of kilometers away from the NMSZ. These occurred ~6,100 yrs BP in the Wabash Valley (Munson *et al*., 1997) and ~ 5,500 yrs BP in eastern Arkansas (Al-Shukri *et al*., 2005). Using a ~2,000-year record of historical seismicity in

North China, Liu *et al*. (2011) documented the absence of a repeating major earthquake at any location in the Wiehe and Shanxi rifts. These observations of multiple events on different faults in the Kutch Rift, at distant locations in the Reelfoot Rift, and non-repeat earthquakes in the rifts in North China are in accord with the unified model wherein different LSCs can be sequentially activated within a rift.

11.9.3 Areal dimensions of local stress changes

Local stress concentrators and the associated surface area affected by S_L are of smaller areal dimensions, with wavelengths of tens to hundreds of kilometers (Table 11.1), that is, an order of magnitude smaller than the areas affected by perturbing secondary regional stresses associated with regional-scale features identified by Zoback (1992a). However, the local stresses S_L associated with these LSCs have magnitudes comparable to S_T as evidenced by the observed rotation of local S_T (next section).

11.9.4 Local rotation of the regional stress field S_T and magnitude of S_L

As discussed in Section 11.5, the interaction of S_L with S_T causes a local rotation in the direction of S_T which depends on the type of LSC, its orientation, and the ratio of the differential horizontal stress to S_L (Figure 11.1). S_L grows with time, and for optimal conditions the rotation γ is detectable from seismicity data. A stress rotation of $>15°$ associated with a perturbing stress suggests that its magnitude is hundreds of megapascals. The various examples of stress rotation (Section 11.5) associated with different LSCs thus suggest that the related stress accumulation on them is adequate to trigger IPEs. The actual magnitude of the stress accumulation will depend on the nature of the LSC, its geometry, and the duration of the stress accumulation.

11.9.5 Local deviatoric stress

Zoback (1992a) presented an example of a secondary deviatoric stress associated with lithospheric thinning in the East African Rift system. Assuming normal frictional and pore pressure distributions, she showed a regional extension in the upper brittle crust of $S_L = -180$ MPa. Mazarbaud *et al*. (2005) presented examples of local extensional deviatoric stress associated with Amorian Massif and Massif Central in northern and central France. Their results suggest that the local stress associated with these LSCs is extensional and of the order of hundreds of megapascals extending over wavelengths of a few hundred kilometers (Table 11.1).

11.9.6 Effect of deglaciation

Perturbing regional secondary stresses act over a large region and interact with local stress changes in the vicinity of LSCs. When this regional perturbing stress is due to elastic

rebound due to deglaciation (GIA) and/or due to erosion, it opposes the ambient regional vertical stress. In some cases the relative value of the vertical stress changes from S_2 to S_3, promoting failure by thrust faulting (see, e.g., Talwani and Rajendran, 1991; Zoback, 1992b; Muir-Wood, 2000; Mazzotti *et al*., 2005; Hurd and Zoback, 2012). Major reverse faulting observed in higher latitudes (e.g., in Fennoscandia) followed the onset of initial deglaciation (Wu, 1998). However, the contribution of GIA to the present-day stress field is less than 10 MPa (Zoback, 1992b; Wu, 1998; Wu and Johnston, 2000). Various authors have suggested that under the present-day stress field the local GIA may be adequate to trigger seismicity on critically stressed faults in Eastern Canada (see, e.g., Quinlan, 1984; Mazzotti *et al*., 2005; Wu and Mazzotti, 2007; Mazzotti and Townend, 2010).

11.10 Discussion

Analysis of newly compiled stress data from Central and Eastern United States and southeastern Canada "suggests that shear failure on the preferred nodal planes generally do not require reduced fault friction or elevated pore pressures" (Hurd and Zoback, 2012). Assuming the normal friction and pore pressure conditions recently confirmed by Hurd and Zoback (2012), Mazzotti and Townend (2010) estimated ~160–250 MPa for the differential stress in the horizontal plane (S_L) for some seismogenic structures in the same study area. These results support the basic premise of the unified model that intraplate earthquakes result primarily from stress build-up of hundreds of megapascals on LSCs. They also argue against models wherein an order of magnitude lower stresses associated with deglaciation, erosion, or thermal and compositional anomalies in the lower crust and upper mantle were proposed to be the cause of intraplate earthquakes. However, these small secondary stresses can modulate S_L due to the LSCs and trigger seismicity.

Next, I discuss some observations related to IPEs and their possible explanations based on the unifying model. These relate to the absence of significant topography in some regions of IPEs, and the apparent absence of detection of anomalous strain accumulation in continental regions.

11.10.1 Absence of topography

In some rift basins there is evidence of uplift of tens to hundreds of meters along internal and border faults. Such is the case in the Kutch Rift Basin, where repeated thrusting along dipping faults that extend to great depths and are oriented almost orthogonally to S_T has led to the formation of local uplifts and grabens (Biswas, 2005; Figure 6.3, this volume). However, the deep-seated, near-vertical faults within the Reelfoot Rift are not favorably oriented relative to S_T, and there is a general lack of extensive topographic expression over extended distances. In the NMSZ thrusting is limited to cross faults and major deformation occurs by strike-slip faulting.

The absence of topography or significant offsets in sedimentary deposits within the Reelfoot Rift has been interpreted to suggest that present-day seismic activity in the NMSZ

is of recent origin (e.g., Grollimund and Zoback, 2001). This interpretation is based on the assumption of repeated earthquakes on a single fault system and ignores the presence of other LSCs within the rift and the effect of erosion. In the presence of several LSCs within a rift system, seismicity is not restricted to any one particular fault, but can jump from one LSC to another (see, e.g., Section 11.9.2 and Figure 11.4). The effect of erosion can also be pronounced. If an earthquake is associated with a scarp, as was the case in 1819, when the M 7.8 earthquake in the Kutch Rift Basin produced a ~4 m high, ~90 km long scarp – the Allah Bund, evidence of it begins to fade due to erosion, and may eventually disappear. Commenting on the flat terrain south of the Allah Bund, where major upheaval had taken place during the earthquake, Frere (1870) wrote: "In some places we were told of small islets of raised ground, which formerly existed on the Runn, and which had been swallowed up, and we were taken to the spot, near Vingur, where such an islet used to stand out from the surface of the Runn. But in no such case did any hollow or chasm remain visible. The islet seemed to have melted down to the general level, and the description given by eye-witnesses of what they saw indicated the action one would expect, from the continued agitation of a mass of wet sand [from earthquakes] surrounded by water." The presence of multiple LSCs within the Reelfoot Rift (Section 11.9.2), and the possible obliteration of minor scarps by erosion over the past several millennia, suggest that tectonism within the Reelfoot Rift may not have been restricted to the Holocene period, but may have had a longer history.

11.10.2 Temporal growth of S_L as a predictor of earthquakes?

According to the unified model, for optimally oriented LSCs, and for any given horizontal stress difference, a temporal increase in S_L manifests itself as an increase in the associated rotation, γ. Conversely, after a major earthquake and a release of the accumulated stress there will be a decrease in both S_L and γ. Currently, with uncertainties in focal mechanisms, the accuracy with which γ can be detected is ~15°. However, in the future, if the direction of the stress field at any location is continuously monitored, it may be theoretically possible to detect temporal changes in γ, and infer a potential growth in S_L as an earthquake precursor.

11.10.3 Apparent absence of strain accumulation

According to the two-dimensional thermo-mechanical continuum model (Hansen and Nielsen, 2003), as well as the unified model, the presence of local stress build-up in the vicinity of LSCs should be associated with local pockets of elevated strain. However, two decades of GPS measurements in the NMSZ have failed to provide a consensus that such pockets of elevated strain rate exist (see, e.g., Newman *et al*., 1999). A possible reason may be that the instrument placement and "our geodetic approach implicitly focuses on motions due to plate wide rather than locally derived stresses" (Newman *et al*., 1999). However, appreciable local pockets of horizontal strain were detected in Kutch, where a dense network of stations was deployed over the aftershock region of the 2001 earthquake and

in the surrounding region (Reddy and Patil, 2008). After the coseismic strain had reduced to background levels, subsequent GPS and InSAR measurements led to the detection of up to ~13 mm/yr of vertical displacement in regions of continuing aftershock activity (Rastogi *et al*., 2012). Another example of localized elevated coseismic epicentral strain was provided by the ~2 m shortening of railroad tracks in the 1886 Charleston earthquake (Talwani, 1999). Kato *et al*. (2009) reported that the 1964 Niigata (M 7.5) and the 1983 Sea of Japan intraplate earthquakes are located in a zone of contractural strain rates larger than 10^{-7}/yr. This elevated strain away from the plate boundary was detected along the Japan Sea coast, on a continuous GPS array (Sagiya *et al*., 2000). The region had been host to the 1964 Niigata (M 7.5), the 1995 Kobe (M 7.2), and four other M > 7.0 earthquakes since 1847 (Sagiya *et al*., 2000).

These observations suggest that in earthquake-prone regions it may be possible to detect preseismic increases in local strain rates, which may indicate potential locations of large earthquakes. A refocus of strain measurement strategy may be in order.

11.11 Conclusions

Intraplate earthquakes account for a very small fraction of the Earth's seismic budget. Although large intraplate earthquakes are much less frequent than their plate-boundary counterparts, when they do occur they can be associated with large-scale destruction. Because of their rarity, efforts to study them have been limited. As the results of these efforts began to accumulate, several features common to intraplate earthquakes were recognized and used to explain their genesis.

In this chapter I present a review of some earlier ideas and integrate them with more recent observations to develop a unified model of intraplate earthquakes. These include a review of both theoretical models and those based on a spatial association of intraplate earthquakes with identifiable geological features. These geological features, located within rigid plates where stresses accumulate in response to a regional compressional stress, S_T, were recognized as LSCs. Pockets of local stress accumulation, S_L, at any LSC extend over wavelengths of tens to hundreds of kilometers and were found to locally change the direction of S_T. At any LSC there is a build-up of S_L which interacts with S_T and may ultimately lead to an intraplate earthquake.

An inventory of M ≥ 4.5 intraplate earthquakes showed that they are preferentially located in old rifts and at boundaries of cratons. Possible reasons for this location preference were suggested by Ziegler (1987), who in his study of inverted basins in central Europe noted, "Amongst different types of intra-plate discontinuities, rifts with strongly thinned crust appear to be prone to early inversion in response to collision related intra-plate tangential stresses. Most wrench faults, which penetrate much of the crust and possibly extend into the upper mantle, are also prone to compressional activation". It thus appears that the location of intraplate earthquakes is not random, but that there is a solid mechanical basis for their preferred location in rifts. Models of basin inversion by Nielsen and Hansen (2000) and Hansen and Nielsen (2003) illustrate these mechanical underpinnings. Ziegler's

(1987) suggestion that deep faults that penetrate the crust can be locations for intraplate deformation could, perhaps, explain the incidence of intraplate earthquakes near craton boundaries. This speculation merits further research.

Detailed analyses of seismicity around LSCs show that the accumulated stress, S_L, affects S_T, locally rotating it over tens to hundreds of kilometers. This suggests that a search for potential locations of large future intraplate earthquakes could be carried out by monitoring evolving S_L on a dense network of seismic and GPS monitors.

Acknowledgements

I want to thank Sue Hough, Randell Stephenson, Tom Owens, and Bill Clendinen for their helpful reviews of various versions of the chapter. I also acknowledge with thanks Scott Howard and Erin Koch for help with the figures. Many of the ideas in this chapter were developed over the years and resulted from fruitful discussions with Kusala Rajendran and Abhijit Gangopadhyay.

References

Adams, J., and Basham, P. (1989). The seismicity and seismotectonics of Canada's eastern margin and craton. In *Earthquakes at North-Atlantic Passive Margins: Neotectonic and Post-Glacial Rebound*, ed. S. Gregersen and P. W. Basham. Boston, MA: Kluwer Academic, pp. 355–370.

Al-Shukri, H. J., Lemmer, R. E., Mahdi, H. H., and Connelly, J. B. (2005). Spatial and temporal characteristics of paleoseismic features in the southern terminus of the New Madrid seismic zone in eastern Arkansas. *Seismological Research Letters*, 76, 502–511.

Andrews, D. J. (1989). Mechanics of fault junctions. *Journal of Geophysical Research*, 94, 9389–9397.

Artyushkov, E. V. (1973). Stresses in the lithosphere caused by crustal thickness inhomogeneities. *Journal of Geophysical Research*, 78, 7675–7708.

Baroux, E., Béthoux, N., and Bellier, O. (2001). Analysis of the stress field in southeastern France from earthquake focal mechanisms. *Geophysical Journal International*, 145, 336–348.

Bisht, R. S. (2011). Major earthquake occurrences in archaeological strata of Harappan Settlement at Dholavira (Kachchh, Gujarat). Abstract No. S16_IGCP I1, *Proceedings of International Symposium on the 2001 Bhuj Earthquake and Advances in Earthquake Science*, AES 2011, ISR, Gandhinagar, p. 112.

Biswas, S. K. (2005). A review of structure and tectonics of Kutch basin, western India, with special reference to earthquakes. *Current Science*, 88, 1592–1600.

Calais, E., Freed, A. M., Van Arsdale, R., and Stein, S. (2010). Triggering of New Madrid seismicity by late-Pleistocene erosion. *Nature*, 466, 608–611.

Campbell, D. L. (1978). Investigation of the stress-concentration mechanism for intraplate earthquakes. *Geophysical Research Letters*, 5, 477–479.

Dentith, M. C., and Weatherstone, W. E. (2003). Controls on intra-plate seismicity in southwestern Australia. *Tectonophysics*, 376, 167–184.

Dziewonsky, A. M., and Anderson, D. L. (1981). Preliminary reference Earth model. *Physics of the Earth and Planetary Interiors*, 25, 297–356.

Ellis, W. L. (1991). Stress distribution in south-central Oklahoma and its relationship to crustal structure and seismicity. In *Rock Mechanics as a Multiple Science*, ed. J.-C. Rogiers. Rotterdam: Balkema, pp. 73–80.

Frere, H. B. E. (1870). Notes on the Runn of Cutch and neighbouring region. *Journal of the Royal Geographical Society London*, 40, 181–207.

Gangopadhyay, A., and Talwani, P. (2003). Symptomatic features of intraplate earthquakes. *Seismological Research Letters*, 74, 863–883.

Gangopadhyay, A., and Talwani, P. (2005). Fault intersections and intraplate seismicity in Charleston, South Carolina: insights from a 2-D numerical model. *Current Science*, 88, 1609–1616.

Gangopadhyay, A., and Talwani, P. (2007). Two-dimensional numerical modeling suggests preferred geometry of intersecting faults. In *Continental Intraplate Earthquakes: Science, Hazard and Policy Issues*, ed. S. Stein and S. Mazzotti. Geological Society of America Special Paper 425, pp. 87–99, doi:10.1130/2007.2425(07).

Gangopadhyay, A., Dickerson, J., and Talwani, P. (2004). A two-dimensional numerical model for current seismicity in the New Madrid Seismic Zone. *Seismological Research Letters*, 75, 406–418.

Grana, J. P., and Richardson, R. M. (1996). Tectonic stress within the New Madrid Seismic zone. *Journal of Geophysical Research*, 101, 5455–5458.

Grollimund, B., and Zoback, M. D. (2001). Did deglaciation trigger intraplate seismicity in the New Madrid seismic zone? *Geology*, 29, 175–178.

Hansen, D. L., and Nielsen, S. B. (2003). Why rifts invert in compression. *Tectonophysics*, 373, 5–24.

Hasagawa, H. S., and Basham, P. W. (1989). Spatial correlation between seismicity and postglacial rebound in eastern Canada. In *Earthquakes at North-Atlantic Passive Margins: Neotectonic and Post-Glacial Rebound*, ed. S. Gregersen and P. W. Basham. Boston, MA: Kluwer Academic, pp. 483–500.

Haxby, W. F., and Turcotte, D. L. (1976). Stresses induced by the addition or removal of overburden and associated thermal effects. *Geology*, 4, 181–184.

Hildenbrand, R. G., Grissom, A., van Schmus, R. S., and Stuart, W. (1996). Quantitative investigations of the Missouri gravity low: a possible expression of a large Late Precambrian batholith intersecting the New Madrid seismic zone. *Journal of Geophysical Research*, 101, 21,921–21,942.

Hildenbrand, T. G., Stuart, W. D., and Talwani, P. (2001). Geologic structures related to New Madrid earthquakes near Memphis, Tennessee, based on gravity and magnetic interpretations. *Engineering Geology*, 62, 105–121.

Horton, S. P., Kim, W.-Y., and Withers, M. (2005). The 6 June 2003 Bardwell, Kentucky earthquake sequence: evidence for a locally perturbed stress field in the Mississippi embayment. *Bulletin of the Seismological Society of America*, 95, 431–445.

Hurd, O., and Zoback, M. D. (2012). Intraplate earthquakes, regional stress and fault mechanics in the central and eastern U.S. and southeastern Canada. *Tectonophysics*, 581, 182–192.

Iio, Y., and Kobayashi, Y. (2002). A physical understanding of large intraplate earthquakes. *Earth, Planets and Space*, 54, 1001–1004.

Iio, Y., Sagiya, T., and Kobayashi, Y. (2004). What controls the occurrence of shallow intraplate earthquakes? *Earth, Planets and Space*, 56, 1077–1086.

Jaeger, J. C., and Cook, N. G. W. (1979). *Fundamentals of Rock Mechanics, 3*. London: Chapman and Hall, p. 591.

Jing, S., and Stephansson, O. (1990). Numerical modelling of intraplate earthquakes by 2-dimensional distinct element method. *Gerlands Beiträge zur Geophysik*, 99, 463–472.

Johnston, A. C. (1989). The seismicity of 'Stable Continental Interiors'. In *Earthquakes at North-Atlantic Passive Margins: Neotectonic and Post-Glacial Rebound*, ed. S. Gregersen and P.W. Basham. Boston, MA: Kluwer Academic, pp. 299–327.

Johnston, A. C., and Kanter, L. R. (1990). Earthquakes in stable continental crust. *Scientific American*, 262, 68–75.

Kane, M. F. (1977). Correlation of major earthquake centers with mafic/ultramafic basement masses. U.S. Geological Survey Professional Paper 1028-O, pp. 199–204.

Kato, A., Kurashimo, E., Igarashi, T., *et al*. (2009). Reactivation of ancient rift system triggers devastating intraplate earthquakes. *Geophysical Research Letters*, 36, L05301, doi:10.1029/2008GL036450.

Kawanishi, R., Iio, Y., Yukutake, Y., Shibutani, T., and Katao, H. (2009). Local stress concentration in the seismic belt along Japan Sea coast inferred from precise focal mechanisms: implications for the stress accumulation process on intraplate faults. *Journal of Geophysical Research*, 114, doi:10.1029/2008JB005765.

Kenner, S. J., and Segall, P. A. (2000). A mechanical model for intraplate earthquakes: application to the New Madrid seismic zone. *Science*, 289, 2329–2332.

King, G. C. P. (1986). Speculations on the geometry of the initiation and termination process of earthquake rupture and its relation to morphological and geological structure. *Pure and Applied Geophysics*, 124, 567–585.

Liu, L., and Zoback, M. D. (1997). Lithospheric strength and intraplate seismicity in the New Madrid seismic zone. *Tectonics*, 16, 585–595.

Liu, M., Stein, S., and Wang, H. (2011). 2000 years of migrating earthquakes in north China: how earthquakes in midcontinents differ from those at plate boundaries. *Lithosphere*, 3, 128–132.

Long, L. T. (1976). Speculations concerning southeastern earthquakes, mafic intrusions, gravity anomalies and stress amplification. *Earthquake Notes*, 47, 29–35.

Mandal, P. (2013). Seismogenesis of the uninterrupted occurrence of the aftershock activity in the 2001 Bhuj earthquake zone, Gujarat, India, during 2001–2010. *Nature Hazards*, 65, 1063–1083.

Mareschal J.-C., and Kuang, J. (1986). Intraplate stresses and seismicity: the role of topography and density heterogeneities. *Tectonophysics*, 132, 153–162.

Mazarbaud, Y., Béthoux, N., Guilbert, J., and Bellier, O. (2005). Evidence for short-scale stress field variations within intraplate central-western France. *Geophysical Journal International*, 160, 161–178.

Mazzotti, S., and Townend, J. (2010). State of stress in central and eastern North America seismic zones. *Lithosphere*, 2, 76–83.

Mazzotti, S., James, T. S., Henton, J., and Adams, J. (2005). GPS crustal strain, post-glacial rebound, and seismic hazard in eastern North America: the Saint Lawrence valley example. *Journal of Geophysical Research*, 110, B11301, doi:10.1029/2004JB003590.

McKeown, F. A. (1978). Hypothesis: many earthquakes in central and southeastern United States are causally related to mafic intrusive bodies. *Journal of Research, U.S. Geological Survey*, 6, 41–50.

Mooney, W. D., Andrews, M. C., Ginzburg, A., Peters, D. A., and Hamilton, R. M. (1983). Crustal structure of the northern Mississippi embayment and a comparison with other rift zones. *Tectonophysics*, 94, 327–348.

Mooney, W. D., Ritsema, J., and Hwang, Y. K. (2012). Crustal seismicity and earthquakes catalog maximum moment magnitude (Mcmax) in stable continental regions (SCRs): correlation with the seismic velocity of the lithosphere. *Earth and Planetary Science Letters*, 357–358, 78–83.

Muir-Wood, R. (2000). Deglaciation seismotectonics: a principal influence on intraplate seismogenesis at high latitudes. *Quaternary Science Reviews*, 19, 1399–1411.

Munson, P. J., Obermeier, S. F., Munson, C. A., and Hajic, M. R. (1997). Liquefaction evidence for Holocene and latest Pliestocene seismicity in southern halves of Indiana and Illinois: a preliminary overview. *Seismological Research Letters*, 68, 521–536.

Newman, A., Stein, S., Weber, J., *et al.* (1999). Slow deformation and lower seismic hazard at the New Madrid seismic zone. *Science*, 284, 619–621.

Nielsen, S. B., and Hansen, D. L. (2000). Physical explanation of the formation and evolution of inversion zones and marginal troughs. *Geology*, 28, 875–878.

Pollitz, F. F., Kellogg, L., and Burgmann, R. (2001). Sinking mafic body in a reactivated lower crust: a mechanism for stress concentration at the New Madrid seismic zone. *Bulletin of the Seismological Society of America*, 91, 1882–1897.

Quinlan, G. (1984). Postglacial rebound and focal mechanisms of eastern Canada earthquakes. *Canadian Journal of Earth Science*, 21, 1018–1023.

Rajendran, K., and Rajendran, C. P. (1998). Characteristics of the 1997 Jabalpur earthquake and their bearing on its mechanism. *Current Science*, 74, 168–174.

Rastogi, B. K., Choudhury, P., Dumka, R., Sreejith, K. M., and Majumdar, T. J. (2012). Stress pulse migration by viscoelastic process for long-distance delayed triggering of shocks in Gujarat, India, after the 2001 M_w 7.7 Bhuj earthquake. In *Extreme Events and Natural Hazards: The Complexity Perspective*, ed. A. S. Sharma, A. Bundle, V. P. Dimri and D. N. Baker. Geophysical Monograph Series, 196, AGU, Washington, D.C., pp. 63–73, doi:10.10.1029/GM196.

Reddy, C. D., and Patil, P. S. (2008). Post-seismic crustal deformation and strain rate in Bhuj region, Western India, after the 2001 January 26 earthquake. *Geophysical Journal International*, 172, 593–606.

Sagiya, T., Miyazaki, S., and Tada, T. (2000). Continuous GPS array and present day crustal deformation of Japan. *Pure and Applied Geophysics*, 157, 2303–2322.

Sandiford, M., and Egholm, D. L. (2008). Enhanced intraplate seismicity along continental margins: some causes and consequences. *Tectonophysics*, 457, 197–208.

Schulte, S., and Mooney, W. (2005). An updated global earthquake catalogue for stable continental regions: reassessing the correlation with ancient rifts. *Geophysical Journal International*, 161, 707–721.

Segall, P., and Pollard, D. D. (1980). Mechanics of discontinuous faults. *Journal of Geophysical Research*, 85, 4337–4350.

Şengör, A. M. C., and Natal'in, B. A. (2005). Rifts of the world. In *Mantle Plumes: Their Identification Through Time*, ed. R. E. Ernst and K. L. Buchan, Geological Society of America Special Paper 352, pp. 389–482.

Sonder, L. J. (1990). Effects of density contrasts on the orientation of stress in the lithosphere: relation to principal stress directions in the Transverse Ranges, California. *Tectonics*, 9, 761–771.

Steffen, H., and Kauffman, G. (2005). Glacial isostatic adjustment of Scandinavia and northwestern Europe and the radial viscosity structure of the earth's mantle. *Geophysical Journal International*, 163, 801–812.

Steffen, R., Eaton, D. W., and Wu, P. (2012). Moment tensors, state of stress and their relation to post-glacial rebound in northeastern Canada. *Geophysical Journal International*, 189, 1741–1752.

Stein, S., Sleep, N., Geller, R. J., Wang, S. C., and Kroeger, C. (1979). Earthquakes along the passive margin of eastern Canada. *Geophysical Research Letters*, 6, 537–540.

Stevenson, D., Gangopadhyay, A., and Talwani, P. (2006). Booming plutons: source of microearthquakes in South Carolina. *Geophysical Research Letters*, 33, L03316, doi:1029/2005 GL 024679.

Stuart, W. D., Hildenbrand, T. G., and Simpson, R. W. (1997). Stressing of the New Madrid seismic zone by lower crustal detachment fault. *Journal of Geophysical Research*, 102, 27623–27633.

Sykes, L. R. (1978). Intra-plate seismicity, reactivation of pre-existing zones of weakness, alkaline magmatism, and other tectonics post-dating continental separation. *Reviews of Geophysics and Space Physics*, 16, 621–688.

Talwani, P. (1988). The intersection model for intraplate earthquakes. *Seismological Research Letters*, 59, 305–310.

Talwani, P. (1999). Fault geometry and earthquakes in continental interiors. *Tectonophysics*, 305, 371–379.

Talwani, P., and Gangopadhyay, A. (2000). Schematic model for intraplate earthquakes. *Eos, Transactions, American Geophysical Union*, 81(48), F 918.

Talwani, P., and Howard, C. S. (2012). January 1, 1913 Union county, South Carolina earthquake, revisited. *South Carolina Geology*, 48, 11–24.

Talwani, P., and Rajendran, K. (1991). Some seismological and geometrical features of intraplate earthquakes. *Tectonophysics*, 186, 19–41.

Turcotte, D. L., and Oxburgh, E. R. (1976). Stress accumulation in the lithosphere. *Tectonophysics*, 35, 183–199.

Vlahovic, G., Powell, C., and Lamontagne, M. (2003). A three-dimensional P wave velocity model for the Charlevoix seismic zone, Quebec, Canada. *Journal of Geophysical Research*, 108, 1–12.

Wu, P. (1998). Intraplate earthquakes and postglacial rebound in eastern Canada and Northern Europe. In *Dynamics of Ice Age Earth: A Nuclear Perspective*, ed. P. Wu. Uetikon-Zurich, Switzerland: Trans Tech Publications, pp. 603–628.

Wu, P., and Johnston, P. (2000). Can deglaciation trigger earthquakes in North America? *Geophysical Research Letters*, 27, 1323–1326.

Wu, P., and Mazzotti, S. (2007). Effects of a lithospheric weak zone on postglacial seismotectonics in eastern Canada and northeastern USA. In *Continental Intraplate Earthquakes: Science, Hazard and Policy Issues*, ed. S. Stein and S. Mazzotti. Geological Society of America Special Paper 425, pp. 113–128, doi:10.1130/2007.2425(09).

Zeigler, P. A. (1987). Late Cretaceous and Cenozoic intra-plate compressional deformations in the Alpine foreland: a geodynamic model. *Tectonophysics*, 137, 389–420.

Zoback, M. L. (1992a). First- and second-order patterns of stress in the lithosphere: The World Stress Map Project. *Journal of Geophysical Research*, 97, 11,703–11,728.

Zoback, M. L. (1992b). Stress field constraints on intraplate seismicity in eastern North America. *Journal of Geophysical Research*, 97, 11,761–11,782.

Zoback, M. L., and Richardson, R. M. (1996). Stress perturbation associated with the Amazonas and other ancient continental rifts. *Journal of Geophysical Research*, 101, 5459–5475.